Title: *GmSALT3* confers shoot Na^+ and Cl^- exclusion in soybean via two distinct processes

Yue Qu[1†], Rongxia Guan[2†], Jayakumar Bose[1], Sam W. Henderson[1], Stefanie Wege[1*], Li-Juan Qiu[2*], Matthew Gilliham[1*]

[1]Australian Research Council Centre of Excellence in Plant Energy Biology, School of Agriculture, Food and Wine & Waite Research Institute, University of Adelaide, Glen Osmond, SA, Australia

[2]The National Key Facility for Crop Gene Resources and Genetic Improvement, Institute of Crop Science, Chinese Academy of Agricultural Sciences, Beijing, China

[*]For correspondence (e-mails matthew.gilliham@adelaide.edu.au; qiulijuan@caas.cn; stephanie.wege@adelaide.edu.au).

[†]These authors have contributed equally to this work.

Funding information

Natural Science Foundation of China, grant number 31830066; Scientific Innovation Project of Chinese Academy of Agricultural Sciences; ARC Centre of Excellence funding CE140100008; ARC Fellowships FT130100709, DE160100804 and DE170100346.

Abstract

Soybean (*Glycine max*) yields are threatened by multiple stresses including soil salinity. *GmSALT3* confers net shoot exclusion for both Na^+ and Cl^- to soybean and improved salt tolerance; however, how the ER-localised GmSALT3 achieves this is unknown. Here, GmSALT3 function was investigated in heterologous systems, and in near isogenic lines that contained the full-length *GmSALT3* gene (NIL-T; salt-tolerant) or a truncated transcript (NIL-S; salt-sensitive). A time course analysis of the NILs confirmed shoot Cl^- exclusion breaks down days prior to Na^+ exclusion. Shoot Na^+ exclusion occurs via a root xylem-based mechanism in NIL-T lines, as is common amongst plants, with Na^+ content significantly greater in NIL-S stem xylem sap. In contrast, NIL-T plants exhibited significantly greater Cl^- content in both the stem xylem and phloem sap compared to NIL-S, indicating that shoot Cl^- exclusion likely depends upon a novel phloem-based Cl^- recirculation back to NIL-T roots. In

heterologous expression systems, GmSALT3 restored growth of K^+-uptake-defective *E. coli*, whilst in *Xenopus laevis* oocytes, GmSALT3 contributed to net influx and accumulation of Na^+, K^+, and Cl^-. Overall, these findings provide new insights on the impact of ER-localised GmSALT3 on plasma membrane ion fluxes and reveals a novel mechanism for shoot Cl^- exclusion.

Highlight

GmSALT3 is a candidate gene that impacts soybean salt tolerance. Here, we found GmSALT3 can affect Na^+, K^+, and Cl^- transport in heterologous systems, and is likely to contribute to soybean ionic toxicity tolerance through phloem-based Cl^- recirculation from shoot and root xylem-based Na^+ exclusion.

Keywords: Salinity tolerance, abiotic stress, soybean, GmSALT3, CHX, ion transporter, shoot ion exclusion

Acknowledgments:

This work was funded by the Natural Science Foundation of China, grant number 31830066 (RG); Scientific Innovation Project of Chinese Academy of Agricultural Sciences (L-J Q). YQ and SH were supported by ARC Centre of Excellence funding awarded to MG (CE140100008). ARC Fellowships supported MG (FT130100709), SW (DE160100804) and JB (DE170100346). We thank Yue (Crystal) Wu for generating the *AtCBL1n* entry vector; Dr. Sunita Ramesh and Assoc. Prof Zhonghua Chen for providing *AtKAT1* construct used in this study; Dr. Gwenda Mayo from Adelaide Microscopy for providing assistance in TEM.

Word count: 6133 (Abstract, Introduction, Methods, Results, Discussion, Acknowledgements)

Introduction

There is a large market demand for soybean (*Glycine max*) as a staple edible oil and food crop; soybean is additionally an important component of intercropping and sequential cropping systems (Singh, 2010). As such, soybean production demand has been projected to increase by nearly 80 percent to 390 Mt by 2050 (Alexandratos & Bruinsma, 2012). However, salinity stress threatens soybean production; soil salinity of 18–20 dS/m (approximately 180 – 200 mM NaCl) has been shown to reduce yield by 61% – from 2261 ± 438 kg/ha under control conditions to 881 ± 260 kg/ha (Chang, Chen, Shao, & Wan, 1994). Nevertheless, not all soybean cultivars are equally as sensitive to salinity stress, with some rare soybean germplasm found to be relatively salt-tolerant. In a large-scale evaluation of soybean salinity tolerance, less than 3% of the 10,128 evaluated soybean germplasm exhibited salt tolerance at both the germination stage and seedling stage, only 83 were found to be highly tolerant to salinity at the vegetative stage only (Shao, Wan, Chang, & Chen, 1993). It has been observed that salt-tolerant soybean cultivars often have superior agronomic performance to salt-sensitive cultivars (Phang, Shao, & Lam, 2008), indicating breeding for stress tolerance soybean may improve overall yields even under standard conditions.

In soybean, a major quantitative trait locus (QTL) for salinity tolerance has been consistently mapped to chromosome 3 (Abel, 1969; Ha et al., 2013; Hamwieh et al., 2011; Hamwieh & Xu, 2008; Lee et al., 2004). Since 2014, several studies have been published focusing on the same dominant gene, identified in this chromosome 3 QTL in wild (*GmCHX1*) and cultivated soybean (*GmNcl*/*GmSALT3*) (Do et al., 2016; Guan et al., 2014; Qi et al., 2014). This gene, *Glyma03g32900* in reference soybean genome of the William 82 variety (William 82. a1.v1.1), is the best candidate for the *Ncl* locus reported by Abel (1969). It should be noted here that in the William 82 genome a2.v1, *Glyma03g32900*, appears to be incorrectly annotated as two transcripts (Glyma.03g171600 and Glyma.03g171700) rather than the full-length coding sequence obtained consistently from cDNA and encoding a full-length CHX protein. Here, we refer to the full-length gene obtained as *GmSALT3*.

According to phylogenetic analyses, the full-length GmSALT3 protein is closely related to *Arabidopsis thaliana* AtCHX20 (a Cation/Proton Exchanger), which is a functionally characterised member of the CPA2 (Cation/Proton Antiporter 2) family of transporters (Guan et al., 2014; Padmanaban et al., 2007). Almost all CHXs that have been functionally characterised have been done so only in heterologous systems. A connection to their roles in plants or their association with phenotypes in loss of function mutants is sparse; GmSALT3 is

92 the only CHX so far connected to salinity tolerance (Sze & Chanroj, 2018). Functional studies
93 of AtCHXs have indicated that they might play role in modulating cation and pH homeostasis
94 within the endomembrane system (Chanroj et al., 2011; Czerny et al., 2016; Padmanaban et al.,
95 2007). The ER-localised AtCHX20 was, for example, suggested to be an endomembrane K^+
96 transporter involved in the osmoregulation of guard cells (Padmanaban et al., 2007).

97 The salt-tolerant soybean cultivar Tiefeng 8 contains a full-length *GmSALT3*, while the
98 salt sensitive cultivar 85-140 contains a 3.78-kb copia retrotransposon insertion in exon 3 of
99 *GmSALT3* that truncates the transcript with a premature stop codon (making the 85-140
100 essentially a *Gmsalt3* knockout). *GmSALT3* is predominantly expressed in root cells associated
101 with the phloem and xylem (Guan et al., 2014); expression of full-length *GmSALT3* in roots
102 leads to reduced shoot accumulation of Na^+ (Guan et al., 2014; Qi et al., 2014) and Cl^- (Liu et
103 al., 2016) and increased crop yield in saline conditions (Do et al., 2016; Liu et al., 2016).
104 GmSALT3 has been localized to the endoplasmic reticulum (ER), similar to AtCHX20. This
105 differs from most other proteins known to be involved in shoot Na^+ and Cl^- exclusion, which
106 have mainly been localised to the plasma membrane and tonoplast.

107 Shoot salt exclusion requires the co-ordinated activity of many ion transporters that
108 may: 1) limit the net entry of salt into the roots, 2) compartmentalise salt in the roots; and or 3)
109 retrieve salt from the root xylem or shoots through the phloem. Examples of transporters that
110 have been implicated in salt tolerance in soybean include: the tonoplast localised GmNHX1
111 (Na^+/H^+ antiporter 1) (Li et al., 2006a); and the plasma membrane localised GmSOS1 (salt
112 overly sensitive 1, Na^+/H^+ antiporter) and GmCAX1 (Ca^{2+}/H^+ antiporter 1) (Luo et al., 2005;
113 Phang et al., 2008). These transporters are proposed to be involved in net exclusion of salt entry
114 into roots (GmSOS1), its compartmentation (*GmNHX1*) or signalling (*GmCAX1*). Significantly,
115 the transporters contributing to reduced net transfer of salt to the shoot, the mechanism by
116 which shoot salt accumulation is commonly regulated in other species, are yet to be resolved
117 in soybean (Cao, Li, Liu, Kong, & Tran, 2018; Munns & Tester, 2008). For instance, in wheat,
118 rice and Arabidopsis the HKT1;5-like (high affinity K^+ transport) proteins that localise to cells
119 that surround the root xylem facilitate Na^+ retrieval back into the root (Rana Munns et al., 2012;
120 Møller et al., 2009; Ren et al., 2005; Uozumi et al., 2000). GmSALT3 differs from these
121 previous proteins in being ER-localised and so is unlikely to directly confer shoot salt exclusion
122 via retrieval from the xylem sap. Therefore, the mechanism by which GmSALT3 imparts
123 improved salt tolerance is yet to be determined.

124 Here, we investigated the function of GmSALT3 in heterologous systems and *in planta*
125 to gain insights into the mechanisms by which GmSALT3 contributes to salt tolerance. In

126 heterologous systems, *GmSALT3* complemented K^+ uptake deficient *Escherichia coli*; while
127 in *Xenopus laevis* oocytes, *GmSALT3* expression resulted in increased net influx of Na^+, K^+
128 and Cl^-. Phenotypes of soybean NILs differing in *GmSALT3* alleles revealed that plants
129 containing full-length *GmSALT3,* compared to truncated *Gmsalt3,* are likely to employ two
130 distinct mechanisms to achieve shoot Na^+ and Cl^- exclusion by facilitating net xylem retrieval
131 of Na^+ and greater phloem Cl^- retranslocation from shoots to roots. As such, we propose that
132 the endomembrane GmSALT3 has a complex physiological role which ultimately impacts
133 multiple ion fluxes across the plasma membrane.
134

135 **Materials and Methods**

136 *Plant materials and growth conditions*

137 Soybean plants were grown in a greenhouse (28 °C day, 16 h light and 25 °C night) at
138 the Plant Research Centre, Waite Campus, University of Adelaide, Australia. Soybean seeds
139 (Tiefeng 8, salt-tolerant parent; 85-140, salt-sensitive parent; NIL-T, near isogenic line with
140 *GmSALT3*; NIL-S, near isogenic line with *Gmsalt3*) were imported from China through
141 quarantine. Soybean seeds were germinated in pots containing a 1:1 mixture of
142 perlite:vermiculite as described by Obermeyer & Tyerman (2005).
143

144 *cDNA cloning and plasmid preparation*

145 To synthesize *GmSALT3* and *Gmsalt3* cDNA (2436 and 1131 nucleotides, respectively),
146 total RNA was isolated from roots of 4-week old soybean plants using the TRIzol method (Shi
147 & Bressan, 2006). First-strand cDNA was synthesized using a Thermoscript RT III kit
148 (Invitrogen, USA). Gene specific primers (GmSALT3_gF and GmSALT3_gR, Gmsalt3_gF
149 and Gmsalt3_gR; Table S1) were used to amplify *GmSALT3* cDNA with Phusion® High-
150 Fidelity DNA Polymerase (New England Biolabs) using 35 cycles (98 °C 30 s, 65 °C 30 s, and
151 72 °C 150 s). Gel-purified PCR products were A-tailed using Taq polymerase (New England
152 Biolabs) for 30 min at 72 °C, and then recombined into Gateway® entry vector
153 PCR8/GW/TOPO (Invitrogen) for subsequent applications. Resulting clones were sequenced
154 using internal primers (GmSALT3_F1, R1, F2, F3, F4, and F5, Gmsalt_F1, F2, and R1; Table
155 S1). The sequence of *GmSALT3-YFP* was PCR amplified from a previously constructed
156 plasmid *pBS-35S::GmSALT3-YFP*; the sequence of *GmSALT3-TM10* (first 10 transmembrane
157 domain of *GmSALT3*) was PCR amplified from *PCR8-GmSALT3*. Gel-purified PCR products

158 of *GmSALT3-YFP, GmSALT3-TM10* were recombined into entry vector PCR8 as described
159 above.
160 *GmSALT3* and *Gmsalt3* CDS, *GmSALT3-YFP, GmSALT3-TM10, AtCHX20 and*
161 *AtKAT1* within entry vector PCR8 were cloned into the pGEM-HE vector and a modified
162 version of pET-DEST42 vector using Gateway ® LR Clonase® (Invitrogen, USA), for *X. laevis*
163 oocyte expression and *E. coli* expression, respectively. The *E. coli* strain TK2463 lacks the T7
164 RNA polymerase, therefore, the T7 promoter in pET-DEST42 was replaced with the TAC
165 promoter. Inverse PCR was performed with 5 ng of plasmid, 50 nM of forward and reverse
166 primer (SH_215 and SH_216, Table S1), and 0.25 units Phusion High Fidelity Polymerase
167 (New England Biolabs) in a final volume of 25 µL. Reactions were treated with Cloning
168 Enhancer (Clontech Laboratories Inc) to remove circular template, and the plasmid was re-
169 circularised using In-Fusion HD enzyme (Clontech Laboratories Inc).
170
171 *Growth assay in Escherichia coli*
172 Competent cell preparation and *E. coli* transformation were conducted as described by
173 Chanroj et al. (2011). The resulting transformants were grown on KML media (10 g/L tryptone,
174 5 g/L yeast extract, 10 g/L KCl) supplemented with 100 µg/mL carbenicillin and incubated at
175 37 ºC overnight; positively transformed colonies were identified by colony PCR with gene
176 specific primers (GmSALT3_gF and _gR; Gmsalt3_gF and gR). For *E. coli* growth
177 experiments, freshly transformed cells were first grown overnight in 5 ml KML at pH 7.2. Cell
178 cultures were replenished (OD_{600} = 0.5) and grown for 3 h in KML, and then washed with low
179 potassium media (10 g/L tryptone, 2 g/L yeast extract, 100 mM D-mannitol) three times. Cells
180 were normalized to OD_{600} 0.5 for a 96-well plate assay. In each well, 20 µL of normalized cell
181 suspension was added to 180 µL growth solutions. All test media were supplemented with 100
182 µg/mL carbenicillin, with or without 0.5 mM IPTG (Isopropyl β-D-1-thiogalactopyranoside).
183 The 96-well plates were inserted into FLUOstar Omega Fluorescence microplate reader (BMG
184 LABTECH) set to 37 ºC and A_{600} was measured every 15 min for 18 h with continuous shaking
185 at 200 rpm.
186
187 *Characterization of GmSALT3 in X. laevis oocytes*
188 pGEMHE-DEST containing *GmSALT3* was linearized using SphI-HF (New England
189 BioLabs); cRNA was synthesized using mMESSAGE mMACHINE T7 Kit (Ambion). 46
190 nL/23 ng of cRNA or equal volumes of RNase-free water were injected into oocytes with a
191 Nanoinject II microinjector (Drummond Scientific). Oocytes were incubated for 48 h in

192 Calcium Ringer's solution (96 mM NaCl, 2 mM KCl, 5 mM $MgCl_2$, 5 mM HEPES, 0.6 mM
193 $CaCl_2$). All solution osmolalities were measured with a Vapor pressure osmometer (Wescor)
194 and adjusted to 240–260 mOsmol kg^{-1} using mannitol. Measurement of ion profiles in oocytes
195 followed Munns et al. (2012) with the following modifications. Six replications of 3 grouped
196 oocytes were used for flame photometry (Sherwood 420), and Cl^- was measured by manual
197 titrimetric Cl^- measurement using a chloride analyser (Sherwood® Chloridometer 926S). For
198 YFP imaging, oocytes were analysed with a Zeiss LSM 5 Pascal Confocal Laser-Scanning
199 Microscope equipped with an argon laser. Excitation/emission conditions for YFP were 514
200 nm/523 to 600 nm.
201
202 *MIFE (Microelectrode Ion Flux Estimation) from oocytes*
203 The MIFE technique allows noninvasive concurrent quantification of net fluxes of
204 several ions using protocols outlined by Shabala et al. (2013) with oocytes being used rather
205 than plant tissues in our experiments; sodium, potassium, and chloride commercial ionophore
206 cocktails (93314, 99311, and 99408, respectively; all from Sigma-Aldrich) were used as LIX
207 (liquid Ion Exchanger) when measuring Na^+, K^+, and Cl^- fluxes. Oocytes were washed in ND96
208 (96 mM NaCl, 1 mM KCl, 1 mM $MgCl_2$, 5 mM HEPES, pH 7.5). After incubation in ND96
209 for 72 hours, fluxes were measured after being transferred to BSM (5 mM NaCl, 0.2 mM KCl,
210 0.2 mM $CaCl_2$, 5 mM HEPES, pH 7.5).
211
212 *TEM (Transmission Electron Microscopy)*
213 Fresh soybean NIL-T and NIL-S roots were sectioned to 1 mm (length), stems were
214 cross sectioned (1 mm in length and 1 mm in radius). Root and stem samples were incubated
215 overnight in 1.5 ml Eppendorf tubes with fixative (2.5% Glutaraldehyde, 4% Formaldehyde,
216 4% Sucrose, 0.1 M Phosphate buffer). Samples were washed three times in 1X PBS and then
217 washed with osmium (263257, Sigma-Aldrich) for 4 hours. Sections were then washed three
218 times in 1X PBS and soaked in 1X PBS for 20 mins and then embedded in 1% agarose gel.
219 Agarose embedded soybean root were cut into blocks (1 cm long). A series of dehydration
220 steps were performed after embedding, using increasing concentrations of ethanol: 50%, 70%,
221 90% and 95% (each for 30 mins), and 100% ethanol for overnight dehydration. Samples were
222 then incubated in increasing concentrations of resin (Spurrs): 5%, 10%, 15%, 20%, 25%, 30%,
223 40%, and 50% (each for 1 h), 50% overnight, 75% (4 h), 100% (4 h), and 100% (overnight).
224 Resin wells containing the agarose blocks were then incubated at 60 ^{o}C for 3 days for

225 polymerization. Polymerised resin capsules were cut to 70 nm thickness using a diamond knife
226 and visualized under transmission electron microscopy (TEM; PHILIPS CM100).
227
228 *NaCl treatment and ion accumulation*
229 Soybean plants were treated with 100 mM NaCl every 2 days (1.5 L solution per tray)
230 at 14 days after sowing; the second dose of 1.5 L 100 mM NaCl was applied 16 days after
231 sowing; the same volume of RO water was applied to the tray of the control plants. Saline
232 solutions or RO water were applied into trays that contain pots with soybean plants. Plant
233 tissues were harvested and dried in oven overnight at 60ºC or freeze-dried overnight. Dry
234 weight was recorded. Then dried samples were digested in 10 mL 1% (v/v) nitric acid overnight
235 at 65ºC or freeze-thawed in Milli-Q water 3 times. Oven-dried samples were utilized to test
236 Na^+ and K^+ accumulation with flame photometry (Sherwood 420), Cl^- was measured by
237 titrimetric Cl^- measurement by using chloride analyser (Sherwood® Chloridometer 926S).
238 Freeze-dried samples were used to measure NO_3 accumulation. The measurement method was
239 modified according to Qiu, Henderson, Tester, Roy, & Gilliham (2016). Supernatant (50 µL)
240 of freeze-dried samples in water was added into 200 µL of 5% (W/V) salicylic acid/H_2SO_4 and
241 incubated at room temperature for 20 min, then 50 µL of this mixture was transferred into 950
242 µL of 2 M NaOH and incubated at room temperature for at least 20 min (to cool down to room
243 temperature). Of this, 250 µL was loaded into separate wells of a flat-bottom transparent 96-
244 well plate (Greiner Bio-One, Austria). Absorbance was measured at 410 nm. Standards
245 measured included 0, 0.5, 1, 2, 2.5, 5, 7.5, and 10 mM KNO_3.
246
247 *Phloem and xylem sap extraction*
248 Phloem sap was extracted according to the method of Rupassara (2008) and Ren et al.
249 (2005). Soybean plant petioles were cut at the base (approx. 0.5 cm above the main stem) and
250 stems were cut approx. 2 cm above ground (upper part), and immediately dipped in 1.5 mL of
251 0.1 mM EDTA solution (pH adjusted to 8 with NaOH) in a 2 mL microcentrifuge tube for 20
252 min, then the tube was immediately dipped in liquid nitrogen and stored in -80 ºC until analysis.
253 The glutamine concentration in the extract was measured using a Glutamine Assay Kit (EGLN-
254 100, EnzyChrom™, BioAssay Systems). Xylem sap was extracted using a pressure chamber.
255 Lower parts of the cut stems with roots were transferred into the pressure chamber. Pressure
256 was increased gradually (0.05 MPa increments) until the xylem sap presented. The first two
257 drops emerging were discarded using a micropipette to reduce contamination from damaged

258 cells or phloem sap (Berthomieu et al., 2003). Xylem sap was then collected during the
259 following 5 min, and stored at -20 ºC until analysis. Ion contents was measured as stated above.
260
261
262 **Results**
263 *GmSALT3 modulates Na^+, K^+, and Cl^- accumulation in soybean*
264 Liu et al. (2016) previously used an extreme salt treatment (200 mM NaCl) that
265 typically results in the death of even the salt tolerant germplasm after a prolonged exposure.
266 Using this method, it was observed that full-length *GmSALT3* improved shoot Na^+ and Cl^-
267 exclusion over 10 days, with higher shoot Cl^- accumulation occurring prior to shoot Na^+
268 accumulation in NIL-S (Liu et al., 2016). Here, we used a lower salt concentration (100 mM)
269 that soybean plants are more likely to encounter in the field and which typically does not result
270 in death of the plants prior to seed production. Furthermore, we studied the time course of Na^+,
271 Cl^- and K^+ accumulation in NIL-T and NIL-S for different leaf types, stems and hypocotyls
272 (Fig. 1). We confirmed that Cl^- accumulates to higher concentrations in NIL-S shoots
273 compared to those of NIL-T (Fig. 1b). Additionally, also without salt treatment, we found a
274 higher Cl^- concentration in NIL-S aerial tissues (leaves and stems) without salt treatment;
275 whereas significantly higher Na^+ accumulation was detected in aerial tissues only after 3 days
276 of NaCl treatment in NIL-S, and higher Cl^- accumulation continued (Fig. 1a,b; Fig. S1, S2).
277 We further observed that K^+ content was increased in NIL-S compared to NIL-T in these tissues
278 following NaCl treatment (Fig. 1c; Fig. S3). The observed accumulation of K^+ showed a similar
279 trend to Na^+, but to a lesser extent, only increasing from 35.7±1.2 mg/g (day 0) to 51.2±1.2
280 mg/g (day 10), compared to 0.3±0.1 mg/g and 45.3±5.6 mg/g for Na^+ in the same period (Fig.
281 1a; 1c). Therefore, although shoot K^+ increased in NIL-S, the ratio of K^+/Na^+ was significantly
282 higher in NIL-T leaves compared to NIL-S when measured after day 3 (Fig. 1d). Salt treatment
283 affected biomass production; after 10 days NaCl treatment the total dry weight of NIL-T was
284 significantly higher, as well as all individual dry weights of leaves, roots, and stem (Fig. 1e, f).
285 After establishing the timeline for shoot ion accumulation in 100 mM NaCl, to ensure
286 we saw differences between the NILs we chose a 4-day time point to further examine where
287 salt was differentially accumulated between NIL-T and NIL-S (Fig. 2, Fig. S4). We examined
288 the ion concentrations in a range of tissue types, and in the vascular sap. After 4 days, Na^+
289 accumulated to a greater extent in all aerial tissues in NIL-S, including leaves (both first
290 trifoliate leaf, FL, and youngest trifoliate leaf, YL), petioles of the first trifoliate leaf (FLP) and

291 youngest trifoliate leaf (YLP), higher stem (HS), lower stem (LS), and Hypocotyl (Hy), which
292 is consistent with what we observed for whole shoot ion content analysis. No significant
293 differences were observed between the NILs for Na^+ in roots under salt treatment (primary root,
294 PR and secondary root, SR; Fig. 2a). Under control conditions (4 days treated with RO water),
295 Na^+ content was significantly more, but still low, in secondary root (SR) of NIL-T compared
296 to NIL-S, with no significant differences in other tissues (Fig. S4). Detailed analysis of the
297 accumulation of K^+ under salt treatment revealed that K^+ was only significantly increased in
298 leaves of NIL-S and not in any other of the investigated aerial tissues or roots (Fig. 2b). No
299 significant differences between NIL-T and NIL-S were observed for K^+ under control
300 conditions (Fig. S4).

301 Under saline conditions, the Cl^- accumulation pattern was similar to that of Na^+
302 accumulation in aerial parts and hypocotyls; more Cl^- accumulated in leaves, stems and
303 hypocotyls of NIL-S compared to NIL-T (Fig. 2c). However, in roots (PR and SR), NIL-T
304 accumulated significantly more Cl^- than NIL-S (Fig. 2c). Under control conditions, Cl^- content
305 was significantly elevated in leaves and stem of NIL-S, with no differences for hypocotyl and
306 roots (Fig. S4). In addition, NO_3^- content was also measured under salt treated conditions and
307 accumulated more in leaves (both FL and YL) and roots in NIL-T compared to NIL-S; the ratio
308 of Cl^- to NO_3^- was significantly lower in NIL-T leaves compared to NIL-S, and no significant
309 difference was observed in roots (Fig. 2d). In summary, significantly less Na^+, K^+, and Cl^-
310 accumulated in NIL-T shoots than NIL-S, which in many plant species is achieved by retention
311 of the ions in the root to avoid accumulation in the xylem sap flow to the shoot. Xylem and
312 phloem sap ion concentrations were therefore determined.

313 Ion concentrations within soybean stem phloem and xylem exudates were examined at
314 the 4-day time point following NaCl treatment. Glutamine contents within the phloem sap was
315 used to normalize these measures to avoid differences in sap volumes leading to artefactual
316 results, as glutamine concentration within the phloem remains constant throughout the day
317 (Corbesier, Havelange, Lejeune, Bernier, & Périlleux, 2001). It was found that the contents of
318 Na^+ and K^+ were not significantly different between the phloem sap of NIL-T and -S plants,
319 but Cl^- concentration was significantly higher in NIL-T stem phloem sap (Fig. 3a). This
320 indicates an increased flow of Cl^- from NIL-T shoots to their roots compared to that found for
321 NIL-S plants; Cl^- is therefore likely to be recirculated from the stem to the roots via the phloem
322 in NIL-T plants. In stem xylem sap, the Na^+ concentration within NIL-S was significantly
323 greater compared to NIL-T, indicating less Na^+ is loaded into the NIL-T xylem – or more is
324 retrieved. Interestingly, in contrast to the accumulation data, the Cl^- concentrations were lower

325 in NIL-S xylem than NIL-T (Fig. 3b). Under control conditions (4 days with RO water), no
326 significant differences were observed between NIL-T and NIL-S for the ion concentrations
327 within stem phloem and xylem sap (Fig. S4d), which may be related to the detection levels of
328 the assays.
329
330 We hypothesized a link between the localization of GmSALT3 in the ER (Guan et al., 2014)
331 and its role in the phloem, as the ER reaches into phloem sieve elements and is directly exposed
332 to the phloem sap (Turgeon & Wolf, 2009). This localisation may enable a direct ion transport
333 from and into the sap of phloem cells and may alter the phloem morphology. In an attempt to
334 investigate this we examined the phloem ultrastructure of three-week old NIL-T and NIL-S
335 roots and stems following 100 mM NaCl treatment for four days. TEM (Transmission Electron
336 Microscopy) imaging did not reveal obvious morphological differences between NIL-T and
337 NIL-S in root phloem cells (Fig. S5), indicating lack of full-length *GmSALT3* does not result
338 in a disruption to sub-cellular morphology.
339
340 *GmSALT3 facilitates Na^+, K^+, and Cl^- transport in heterologous systems*
341 We functionally characterised GmSALT3 in heterologous systems, including the *E.*
342 *coli* strain TK2463 (*trkAΔ, kup1Δ, kdpABCDEΔ*), which is defective in native K^+ uptake
343 mechanisms (Epstein, Buurman, McLaggan, & Naprstek, 1993) (Fig. 4) and shows a reduced
344 growth trajectory in media with low K^+ (Epstein et al., 1993). In low K^+-containing medium
345 (~2 mM K^+), IPTG (Isopropyl β-D-1-thiogalactopyranoside)-induced expression of full length
346 *GmSALT3* in TK2463 improved its growth compared to bacteria expressing the truncated
347 *Gmsalt3* and the negative control (AtCBL1n, a 12 aa peptide with the sequence
348 MGCFHSKAAKEF; Batistič, Waadt, Steinhorst, Held, & Kudla, 2010) (Fig. 4a; 4b).
349 Arabidopsis AtCHX20 (Chanroj et al., 2011) and AtKAT1 (Anderson, Huprikar, Kochian,
350 Lucas, & Gaber, 1992), a known plasma membrane potassium channel from Arabidopsis, were
351 included as positive controls, and showed similar or superior growth to the *GmSALT3*-
352 expressing bacteria (Fig. 4a; 4b). As we had previously used GmSALT3-YFP for determining
353 the subcellular localisation of GmSALT3 (Guan et al., 2014), we investigated if this
354 translational fusion of GmSALT3 with YFP on the C-terminus is functional and could
355 complement TK2463 *E. coli*. Additionally, we were interested if the last transmembrane
356 domain of GmSALT3 is important for functionality - truncated *Gmsalt3* from NIL-S contains
357 only 9 out of the 10 predicted alpha-helices. We therefore constructed GmSALT3-TM10, that
358 has all 10 TM alpha -helices with only the hydrophilic C-terminus removed. Both, YFP-tagged

359 GmSALT3 and GmSALT3-TM10 increased *E. coli* growth to that of GmSALT3 and
360 significantly greater than that of Gmsalt3 (Fig. 4a; 4b). None of the test constructs or controls
361 used had a significant impact on bacterial growth rates on media high K^+ (Fig. S6); on media
362 with low K^+ and no IPTG GmSALT3 did not show any significant growth differences from
363 Gmsalt3 which was no different from the negative control (Fig. S6). In summary, bacterial
364 growth assays suggest that in addition to GmSALT3, YFP-tagged GmSALT3 and GmSALT3-
365 TM10 are functional. This indicates all transmembrane domains are important for GmSALT3
366 transport function, but the large (383 aa) hydrophilic C-terminus can be truncated or added to
367 without abolishing K^+ transport.

368 As the presence of functional GmSALT3 in soybean causes shoot ion exclusion for Na^+,
369 Cl^- and K^+, we were interested to see if the presence of the protein in cells influences the flux
370 of all three ions across the PM. To investigate this, we expressed YFP-tagged and untagged
371 GmSALT3 in *X. laevis* oocytes. Although GmSALT3 is localised to the ER in plant cells and
372 no PM-localisation was observed (Guan et al., 2014), we detected fluorescence at the PM in
373 *GmSALT3*-YFP expressing oocytes, similar to the fluorescence of oocytes expressing the PM-
374 localised positive control *TmHKT1;5-A*-YFP (Fig. 5a) (*Triticum monococcum* High-Affinity
375 K^+ Transporter 1; Munns et al., 2012). It is not uncommon for plant endomembrane proteins
376 to at least partially localise to the PM in frog oocytes (Maurel, Reizer, Schroeder, & Chrispeels,
377 1993). Two electrode voltage-clamp electrophysiology revealed that the resting membrane
378 potential of *GmSALT3*-injected oocytes was more positive compared to H_2O-injected oocytes
379 when incubated in ND96 media (Fig. 5b), but no consistent current differences were detected.
380 Therefore, we chose to conduct MIFE (Microelectrode Ion Flux Estimation) experiments to
381 measure ion fluxes. MIFE results indicated that in *GmSALT3*-injected oocytes net efflux of
382 Na^+, K^+, and Cl^- was reduced compared to H_2O-injected oocytes (Fig. 5c). Ion content analysis
383 of oocytes revealed that, in agreement with the reduced net ion efflux in oocytes, *GmSALT3*-
384 injected oocytes contained significantly more K^+, Na^+, and Cl^- compared to H_2O-injected
385 oocytes (Fig. 5d). To test whether GmSALT3 induced differences in ion concentration could
386 be blocked in oocytes, we used the Na^+ channel and Na^+/H^+ exchanger inhibitor amiloride
387 hydrochloride (Darley et al., 2000). Oocytes were transferred from ND96 to BSM (low Na^+,
388 K^+ and Cl^-) and incubated overnight. Oocytes incubated without amiloride, showed a smaller
389 relative K^+, Na^+, and Cl^- content decrease in *GmSALT3*-injected oocytes compared to H_2O-
390 injected oocytes as expected (Fig. 5d). However, no difference was observed between control
391 and *GmSALT3*-injected oocytes when the Na^+ transporter inhibitor amiloride was present (Fig.
392 5d), confirming GmSALT3 could affect transport of K^+, Na^+, and Cl^- across the PM in oocytes.

393 **Discussion**

394 **The effect of GmSALT3 on ion accumulation *in planta* following salt treatment**

395 Salt resistance includes tolerance to elevated levels of both Cl^- and Na^+. In many plant
396 species one of the two ions is more deleterious to the plant, however, the situation for soybean
397 is currently unclear with evidence for both ions being more toxic than the other (Läuchli, 1984).
398 Whilst our work does not answer which ion causes the most damage to soybean, it does clearly
399 demonstrate that Na^+ and Cl^- long distance transport, and its accumulation in shoots, is
400 uncoupled in soybean. It is clear that Na^+ and Cl^- long distance transport is under the control
401 of distinct mechanisms even if the same gene appears to impact the transport of both ions. We
402 gathered the evidence to demonstrate this when we treated plants with 100 mM NaCl to mimic
403 a more physiologically relevant salt treatment than has previously been used on NIL plants (i.e.
404 one that would be found in the field). We confirmed in these conditions that shoot exclusion
405 of Cl^- broke down prior to exclusion of Na^+ in NIL-S when compared with NIL-S plants (Fig.
406 1).

407 Na^+ and Cl^- are transported to shoots via the xylem transpiration stream. Under saline
408 conditions, Na^+ was accumulated to greater concentrations in the aerial parts of NIL-S but no
409 difference was observed in the roots compared to NIL-T (Fig. 2b); in stem xylem sap, there
410 was a lower Na^+ concentration in NIL-T compared to NIL-S but no significant difference in
411 stem phloem sap (Fig. 3). This indicates more Na^+ is transported in the NIL-S xylem stream.
412 As such net loading of Na^+ to NIL-T xylem is likely to be restricted compared to NIL-S plants.
413 As for Cl^-, more Cl^- is transported to the shoots in NIL-T xylem, but it clearly does not stay in
414 there, instead, the higher phloem sap concentrations indicate that Cl^- most likely is recirculated
415 to the root (Fig 3). *GmSALT3* might therefore impact Cl^- distribution in the plant via phloem
416 recirculation of Cl^-, resulting eventually in higher Cl^- accumulation in NIL-T roots. In addition,
417 when irrigated with RO (Reverse osmosis) water, NIL-S plants had significantly higher
418 accumulation of Cl^- in aerial tissues (leaves and stems) than NIL-T plants, indicating an
419 intrinsic difference in net loading of the shoot even under non-saline conditions (Fig. S4). No
420 differences in phloem Cl^- concentration or shoot Na^+ content could be detected under these
421 control conditions which is possibly the result of the low signal for each parameter and
422 differences might fall under the detection limit of the method (Fig. S4). These data clearly show
423 there are distinct mechanisms operating for the control of long-distance transport of Na^+ and
424 Cl^-.

425 NO_3^- has previously been shown to be an effective competitor of Cl^- uptake to alleviate
426 ion toxicities in soybean under salt stress, indicating that leaf Cl^-/NO_3^- ratio may be a
427 significant index for evaluating salt tolerance, as with K^+/Na^+ (Guo, Zhou, Li, Yu, & Luo,
428 2017). After salt treatment (100 mM for 4 days), NIL-T had a much lower Cl^-/NO_3^- ratio in
429 leaves than NIL-S (Fig. 2d), indicating that NIL-T may reduce potential chloride toxicity in
430 shoots by maintaining a low Cl^-/NO_3^- ratio (Li et al., 2017; Wege, Gilliham & Henderson,
431 2017).
432 In NIL-S, without GmSALT3, K^+ concentration in shoots increased during the salt
433 treatment (simultaneously with Na^+), this did not occur in NIL-T (Fig. 1c), and might be a
434 compensatory effect in NIL-S to maintain a higher K^+/Na^+ ratio. Interestingly, NIL-T leaves
435 maintained a constant K^+ concentration throughout ten days of salt treatment even though Na^+
436 and Cl^- increased after salt treatment (Fig. 1). No significant difference could be detected for
437 K^+ concentration between roots of NIL-T and NIL-S plants (Fig. 2c). This indicates that
438 GmSALT3 also affects shoot K^+ accumulation in soybean.
439
440 **Transport function of GmSALT3**
441 Based on the ER-localisation of GmSALT3 (Guan et al., 2014) and the complex and
442 distinct processes underlying the different salt ion accumulation phenotypes of the two NILs,
443 we propose that GmSALT3 affects processes at the ER and is not directly mediating ion
444 transport across the PM or tonoplast itself – this makes it unlike most other transport proteins
445 identified as important for salt tolerance.
446 A close homolog of *GmSALT3*, *AtCHX20* in *Arabidopsis thaliana*, is preferentially
447 expressed in stomatal guard cells, and also localises to the ER like GmSALT3, with an ER-
448 localised GFP-tagged version complementing the *Atchx20* knockout phenotype (Padmanaban
449 et al., 2007). *AtCHX20* was shown to enhance growth of *E. coli* deficient in K^+ uptake (LB2003)
450 (Chanroj et al., 2011). We confirmed this result with a different K^+ transport deficient *E. coli*
451 strain (TK2463), and showed that GmSALT3 had a similar effect on *E. coli* growth as
452 AtCHX20.
453 Plant CPA2 (Cation-Proton Antiporter 2)/CHX (Cation/H^+ Exchangers) have not been
454 characterised in *X. laevis* oocytes before, different from some CPA2 members from the animal
455 field. Two *Drosophila* CPA2 transporters, NHA1 and NHA2, have been suggested to act as a
456 Na^+/H^+ exchanger and a H^+/Cl^- cotransporter, respectively (Chintapalli et al., 2015), suggesting
457 that proteins from this family can putatively act as either, cation or anion transporters. Unlike
458 *in planta*, GmSALT3 targeted, at least partially, to the PM of *X. laevis* oocytes (Fig. 5a).

459 GmSALT3 protein expression led to a depolarization of the membrane potential, similar to
460 what was reported for NHA injected oocytes (Chintapalli et al., 2015). We also observed
461 *GmSALT3* expression in oocytes led to a lower net ion efflux of all three ions, K^+, Na^+ and Cl^-
462 (Fig. 5c). Interestingly, the reduced efflux effect was inhibited with the Na^+ channel and Na^+/H^+
463 exchanger inhibitor amiloride hydrochloride. Whilst this inhibitor is thought to be selective for
464 Na^+ transporters, it had an impact on the efflux rate of all three ions measured, Na^+, K^+ and Cl^-.
465 It is possible that observed differences in ion flux and accumulation in heterologous systems
466 are the result of changing cytosolic ion concentration which then impacts ion gradients across
467 the PM and influences the activity of native ion transporters. In such a scenario the fluxes
468 detected across the PM of oocytes is the combination of GmSALT3 and native transporters;
469 and the inhibition of one component leads to the inhibition of the entire mechanism.
470

471 **Putative *in planta* mechanisms for GmSALT3 regulating long distance ion transport**

472 We propose that *in planta* ER-localised GmSALT3 influences ion gradients across the
473 PM through currently unknown downstream effects. This might be through impacting the
474 activity of PM-localised transporters, by changing their PM-abundance or changing cytosolic
475 ion supply, or even more complex effects. For example, if the ionic milieu within the ER is
476 affected this could impact the function or sorting of other membrane transporters or regulatory
477 proteins, which then impacts PM fluxes. Such a mechanism has been suggested for prevacuolar
478 compartment (PVC) localised AtCHX17 and ER localised AtCHX20 (Chanroj et al., 2011).
479 The complexity of this novel salt tolerance mechanisms is further highlighted by the previous
480 observation that root GmSALT3 is sufficient to mediate shoot salt exclusion, using NIL-T and
481 NIL-S grafts (Guan et al., 2014). Further experiments will need to be carried out to decipher
482 the novel mechanism imparted by GmSALT3 that is important for salt tolerance. This might
483 enable us to identify similar mechanisms in other (crop) plants.

484 Phloem translocation of Cl^- appears to be conferred by GmSALT3. Phloem
485 retranslocation of NaCl in saline conditions has been observed before, for example, it was
486 found that in maize approximately 13-36% of the Na^+ and Cl^- imported to leaves through the
487 xylem was retranslocated to the root again in the phloem (Lohaus et al., 2000). However, no
488 transport protein could be linked to this phenomenon. Until now, no reports have shown
489 phloem recirculation of Cl^- to be an important salt tolerance mechanism; *GmSALT3* presents
490 as a very promising candidate for impacting Cl^- long-distance re-translocation.
491

492 **Conclusion**

493 To summarize, this work has provided further insights into the salinity tolerance
494 mechanisms imparted by GmSALT3 *in planta* and in heterologous systems. We propose that,
495 in NIL-T, the presence of full-length *GmSALT3* mediates Na^+ and Cl^- exclusion from shoots
496 through restricting net xylem loading of Na^+, while Cl^- is retranslocated from the shoots back
497 into the roots via the phloem. In heterologous systems, GmSALT3 is involved in K^+ uptake in
498 *E. coli* cells, and its expression in *X. laevis* oocytes mediates net import of Na^+, K^+, and Cl^-.
499 However, as it is an endomembrane-localised protein, how GmSALT3 contributes to soybean
500 salinity tolerance mechanisms is still not clear, and how its expression directly impacts salt
501 movement to and from shoots is unresolved. As the heterologous expression of *GmSALT3* led
502 to transport differences in all three ions that are affected in distribution in the plant it is tempting
503 to speculate that GmSALT3 may be actively involved in their distribution in tissues. However,
504 as the effect on Cl^- and Na^+ in the xylem and phloem differs, the impact of other processes
505 including other transport proteins are likely to be involved in the NIL phenotypes. RNA-
506 sequencing using NIL-T and NIL-S roots may be beneficial in investigating if GmSALT3
507 confers salinity tolerance in soybean roots via influencing transcription, and what distinctive
508 pathways and genes have been significantly changed in NIL-T and NIL-S roots under saline
509 conditions.
510
511 **Acknowledgements**
512 We thank Yue (Crystal) Wu for generating the *AtCBL1n* entry vector; Sunita Ramesh
513 and Zhonghua Chen for providing *AtKAT1* construct used in this study; CSIRO, Australia for
514 donating *E. coli* strain TK2463. We thank Adelaide Microscopy, especially Gwenda Mayo for
515 the use of TEM and other imaging facilities. This work was funded by the Natural Science
516 Foundation of China, grant number 31830066 (RG). YQ and SH were supported by ARC
517 Centre of Excellence funding awarded to MG (CE140100008). ARC Fellowships supported
518 MG (FT130100709), SW (DE160100804) and JB (DE170100346).
519
520 **Author contributions**
521 MG, YQ and SW designed experiments, with input from LQ and RG. LQ and MG
522 directed the project. YQ performed ion accumulation measurement, TEM, IRGA, *E. coli* and
523 oocyte expression, analysed the data and drafted the manuscript. JB performed MIFE in
524 oocytes. SH assisted with experimental design and provided the *E. coli* expression vectors. YQ,
525 MG and SW edited the manuscript. All authors commented on the manuscript.

References

Abel G. (1969). Inheritance of the capacity for chloride inclusion and chloride exclusion by soybeans. *Crop Science*, 9, 697-698.

Alexandratos N. & Bruinsma J. (2012). World agriculture towards 2030/2050: the 2012 revision: ESA Working paper No.12-03. Rome, FAO.

Anderson J.A., Huprikar S.S., Kochian L.V., Lucas W.J. & Gaber R.F. (1992). Functional expression of a probable *Arabidopsis thaliana* potassium channel in *Saccharomyces cerevisiae*. *Proceedings of the National Academy of Sciences*, 89, 3736-3740.

Batistič O., Waadt R., Steinhorst L., Held K. & Kudla J. (2010). CBL-mediated targeting of CIPKs facilitates the decoding of calcium signals emanating from distinct cellular stores. *The Plant Journal*, 61, 211-222.

Berthomieu P., Conéjéro G., Nublat A., Brackenbury W.J., Lambert C., Savio C., Uozumi N., Oiki S., Yamada K. & Cellier F. (2003). Functional analysis of AtHKT1 in Arabidopsis shows that Na^+ recirculation by the phloem is crucial for salt tolerance. *The EMBO Journal*, 22, 2004-2014.

Cao D., Li Y., Liu B., Kong F., & Tran L.S.P. (2018). Adaptive mechanisms of soybean grown on salt-affected soils. *Land degradation & development*, 29(4), 1054-1064.

Chang R.Z., Chen Y.W., Shao G.H., Wan C.W. (1994). Effect of salt stress on agronomic characters and chemical quality of seeds in soybean. *Soybean Science*, 13, 101-105.

Chanroj S., Lu Y., Padmanaban S., Nanatani K., Uozumi N., Rao R. & Sze H. (2011). Plant-specific cation/H^+ exchanger 17 and its homologs are endomembrane K^+ transporters with roles in protein sorting. *Journal of Biological Chemistry*, 286, 33931-33941.

Chintapalli V.R., Kato A., Henderson L., Hirata T., Woods D.J., Overend G., Davies S.A., Romero M.F. & Dow J.A. (2015). Transport proteins NHA1 and NHA2 are essential for survival, but have distinct transport modalities. *Proceedings of the National Academy of Sciences*, 112, 11720-11725.

Corbesier L., Havelange A., Lejeune P., Bernier G. & Périlleux C. (2001). N content of phloem and xylem exudates during the transition to flowering in *Sinapis alba* and *Arabidopsis thaliana*. *Plant, Cell & Environment*, 24, 367-375.

Czerny D.D., Padmanaban S., Anishkin A., Venema K., Riaz Z. & Sze H. (2016). Protein architecture and core residues in unwound α-helices provide insights to the function of a plant transporter AtCHX17. *Biochimica et Biophysica Acta (BBA)-Biomembranes,* 1858, 1983-1998.

559 Do T.D., Chen H., Hien V.T.T., Hamwieh A., Yamada T., Sato T., Yan Y., Cong H., Shono
560 M. & Suenaga K. (2016). Ncl synchronously regulates Na^+, K^+, and Cl^- in soybean and
561 greatly increases the grain yield in saline field conditions. *Scientific Reports*, 6, 19147.
562 Epstein W., Buurman E., McLaggan D. & Naprstek J. (1993). Multiple mechanisms, roles and
563 controls of K^+ transport in *Escherichia coli*: Portland Press Limited.
564 FAO. (2017). *The future of food and agriculture – Trends and challenges*, Rome: FAO.
565 Gilliham M., Able J.A. & Roy S.J. (2017). Translating knowledge about abiotic stress tolerance
566 to breeding programmes. *The Plant Journal*. 90, 898-917.
567 Guan R., Qu Y., Guo Y., Yu L., Liu Y., Jiang J., Chen J., Ren Y., Liu G. & Tian L. (2014).
568 Salinity tolerance in soybean is modulated by natural variation in *GmSALT3*. *The Plant*
569 *Journal*, 80, 937-950.
570 Guo J., Zhou Q., Li X., Yu B. & Luo Q. (2017). Enhancing NO_3^- supply confers NaCl tolerance
571 by adjusting Cl^- uptake and transport in *G. max* & *G. soja*. *Journal of Soil Science and*
572 *Plant Nutrition*, 17, 194-202.
573 Ha B.K., Vuong T.D., Velusamy V., Nguyen H.T., Shannon J.G. & Lee J.D. (2013). Genetic
574 mapping of quantitative trait loci conditioning salt tolerance in wild soybean (*Glycine*
575 *soja*) PI 483463. *Euphytica*. 193, 79-88.
576 Hamwieh A., Tuyen D.D., Cong H., Benitez E.R., Takahashi R. & Xu, D.H. (2011).
577 Identification and validation of a major QTL for salt tolerance in soybean. *Euphytica,*
578 179:,451-459.
579 Hamwieh A. & Xu D. (2008). Conserved salt tolerance quantitative trait locus QTL) in wild
580 and cultivated soybeans. *Breeding Science*, 58, 355-359.
581 Ikeda M. (2005). Distribution of K^+, Na^+ and Cl^- in root and leaf cells of soybean and cucumber
582 plants grown under salinity conditions. *Soil Science and Plant Nutrition*, 51, 1053-1057.
583 Lee G.J., Carter J.T.E., Villagarcia M.R., Li Z., Zhou X., Gibbs M.O. & Boerma H.R. (2004).
584 A major QTL conditioning salt tolerance in S-100 soybean and descendent cultivars.
585 *Theoretical and Applied Genetics*, 109, 1610-1619.
586 Lenis J., Ellersieck M., Blevins D., Sleper D., Nguyen H., Dunn D., Lee J. & Shannon J. (2011).
587 Differences in ion accumulation and salt tolerance among *Glycine* accessions. *Journal*
588 *of Agronomy and Crop Science*. 197, 302-310.
589 Li B., Tester M. & Gilliham M. (2017). Chloride on the Move. *Trends in Plant Science*, 22,
590 236-248.

591 Li W.Y., Wong F.L., Tsai S.N., Phang T.H., Shao G. & Lam H.M. (2006a). Tonoplast-located
592 *GmCLC1* and *GmNHX1* from soybean enhance NaCl tolerance in transgenic bright
593 yellow (BY)-2 cells. *Plant Cell & Environment*, 29, 1122-1137.
594 Li X.J., An P., Inanaga S., Eneji A.E. & Tanabe K. (2006b). Salinity and defoliation effects on
595 soybean growth. *Journal of Plant Nutrition*, 29, 1499-1508.
596 Liu Y., Yu L., Qu Y., Chen J., Liu X., Hong H., Liu Z., Chang R., Gilliham M., Qiu L. & Guan
597 R. (2016). GmSALT3, which confers improved soybean salt tolerance in the field,
598 increases leaf Cl^- exclusion prior to Na^+ exclusion but does not improve early vigor
599 under salinity. *Frontiers in Plant Science*, 7, 1485
600 Lohaus G., Hussmann M., Pennewiss K., Schneider H., Zhu J.J. & Sattelmacher B. (2000).
601 Solute balance of a maize (*Zea mays* L.) source leaf as affected by salt treatment with
602 special emphasis on phloem retranslocation and ion leaching. *Journal of Experimental*
603 *Botany*, 51, 1721-1732.
604 Luo G.Z., Wang H.W., Huang J., Tian A.G., Wang Y.J., Zhang J.S. & Chen S.Y. (2005a). A
605 putative plasma membrane cation/proton antiporter from soybean confers salt tolerance
606 in Arabidopsis. *Plant Molecular Biology*, 59, 809-820.
607 Luo Q., Yu B. & Liu Y. (2005b). Differential sensitivity to chloride and sodium ions in
608 seedlings of *Glycine max* and *G. soja* under NaCl stress. *Journal of Plant Physiology*,
609 162, 1003-1012.
610 Läuchli A. (1984). Salt exclusion: An adaptation of legumes for crops and pastures under saline
611 conditions. In *Salinity Tolerance in Plants: Strageiges for Crop Improvement* (Staples,
612 R.C. and Toenniessen, G.H. eds). New York: Wiley, pp. 171-187.
613 Maurel C., Reizer J., Schroeder J.I. & Chrispeels M.J.. (1993). The vacuolar membrane protein
614 gamma-TIP creates water specific channels in *Xenopus oocytes*. *The EMBO Journal*,
615 12, 2241-2247.
616 Munns R. & Gilliham M. (2015). Salinity tolerance of crops–what is the cost? *New Phytologist*,
617 208, 668-673.
618 Munns R., James R.A., Xu B., Athman A., Conn S.J., Jordans C., Byrt C.S., Hare R.A.,
619 Tyerman S.D. & Tester M. (2012). Wheat grain yield on saline soils is improved by an
620 ancestral Na^+ transporter gene. *Nature Biotechnology*, 30, 360-364.
621 Munns R. & Tester M. (2008). Mechanisms of salinity tolerance. *Annural Review Plant*
622 *Biology*, 59, 651-681.

623 Møller I.S., Gilliham M., Jha D., Mayo G.M., Roy S.J., Coates J.C., Haseloff J. & Tester M.
624 (2009). Shoot Na^+ exclusion and increased salinity tolerance engineered by cell type-
625 specific alteration of Na^+ transport in *Arabidopsis*. *Plant Cell*, 21, 2163-2178.
626 Obermeyer G. & Tyerman S.D. (2005). NH_4^+ currents across the peribacteroid membrane of
627 soybean. Macroscopic and microscopic properties, inhibition by Mg^{2+}, and temperature
628 dependence indicate a SubpicoSiemens channel finely regulated by divalent cations.
629 *Plant Physiology*, 139, 1015-1029.
630 Padmanaban S., Chanroj S., Kwak J.M., Li X., Ward J.M. & Sze H. (2007). Participation of
631 endomembrane cation/H^+ exchanger *AtCHX20* in osmoregulation of guard cells. *Plant*
632 *Physiology*, 144, 82-93.
633 Phang T.H., Shao G. & Lam H.M. (2008). Salt tolerance in soybean. *Journal of Integrative*
634 *Plant Biology*, 50, 1196-1212.
635 Phang T.H., Shao G., Liao H., Yan X. & Lam H.M. (2009). High external phosphate (Pi)
636 increases sodium ion uptake and reduces salt tolerance of 'Pi-tolerant'soybean.
637 *Physiologia Plantarum*, 135, 412-425.
638 Qi X., Li M.W., Xie M., Liu X., Ni M., Shao G., Song C., Yim A.K.Y., Tao Y., Wong F.L. &
639 Isobe S. (2014). Identification of a novel salt tolerance gene in wild soybean by whole-
640 genome sequencing. *Nature Communications*, 5, 4340.
641 Qiu J., Henderson S.W., Tester M., Roy S.J. & Gilliham M. (2016). SLAH1, a homologue of
642 the slow type anion channel SLAC1, modulates shoot Cl^- accumulation and salt
643 tolerance in *Arabidopsis thaliana*. *Journal of Experimental Botany*, 67, 4495-4505.
644 Ren Z.H., Gao J.P., Li L.G., Cai X.L., Huang W., Chao D.Y., Zhu M.Z., Wang Z.Y., Luan S.
645 & Lin H.X. (2005). A rice quantitative trait locus for salt tolerance encodes a sodium
646 transporter. *Nature Genetics*, 37, 1141-1146.
647 Roy S.J., Negrão S. & Tester M. (2014). Salt resistant crop plants. *Current Opinion in*
648 *Biotechnology*, 26, 115-124.
649 Rupassara S.I. (2008). *Metabolite profiling of leaves and vascular exudates in soybean grown*
650 *under free-air concentration enrichment*. University of Illinois at Urbana-Champaign.
651 Rus A., Baxter I., Muthukumar B., Gustin J., Lahner B., Yakubova E. & Salt D.E. (2006).
652 Natural variants of AtHKT1 enhance Na^+ accumulation in two wild populations of
653 *Arabidopsis*. *PLoS Genetics*, 2, 210.
654 Shabala S., Shabala L., Bose J., Cuin T. & Newman I. (2013). Ion flux measurements using
655 the MIFE technique. *Plant Mineral Nutrients: Methods and Protocols*, 171-183.

656 Shao G.H., Wan C.W., Chang R.Z. & Chen Y.W. (1993). Preliminary study on the damage of
657 plasma membrane caused by salt stress. *Crops,* 1, 39-40.
658 Shi H., Bressan R.. (2006). RNA extraction. *Methods in Molecular Biology* 323: 345.
659 Singh G. (2010). *The soybean: botany, production and uses* Oxfordshire, UK: CABI
660 Publishing.
661 Sze H. & Chanroj S. (2018). Plant endomembrane dynamics: Studies of K^+/H^+ antiporters
662 provide insights on the effects of pH and ion homeostasis. *Plant Physiology*, 177:875-
663 95.
664 Tester M. & Davenport R. (2003). Na^+ tolerance and Na^+ transport in higher plants. *Annals of*
665 *Botany*, 91, 503-527.
666 Tester M. & Langridge P. (2010). Breeding technologies to increase crop production in a
667 changing world. *Science*, 327, 818-822.
668 Tian H., Baxter I.R., Lahner B., Reinders A., Salt D.E. & Ward J.M. (2010). Arabidopsis
669 NPCC6/NaKR1 is a phloem mobile metal binding protein necessary for phloem
670 function and root meristem maintenance. *The Plant Cell*, 22, 3963-3979.
671 Turgeon R. & Wolf S. (2009). Phloem transport: cellular pathways and molecular trafficking.
672 In *Annual Review of Plant Biol*ogy, 60, 207-221.
673 Uozumi N., Kim E.J., Rubio F., Yamaguchi T., Muto S., Tsuboi A., Bakker E.P., Nakamura T.
674 & Schroeder J.I. (2000). The Arabidopsis *HKT1* gene homolog mediates inward Na^+
675 currents in *Xenopus laevis* oocytes and Na^+ uptake in *Saccharomyces cerevisiae*. *Plant*
676 *Physiology,* 122, 1249-1260.
677 Wege S., Gilliham M. & Henderson, S.W. (2017). Chloride: not simply a 'cheap osmoticum',
678 but a beneficial plant macronutrient. *Journal of Experimental Botany*, 68, 3057-3069.
679 Xu G.H., Magen H., Tarchitzky J. & Kafkafi U. (2000). Advances in chloride nutrition of
680 plants. San Diego: Academic Press Inc., pp. 97-150.
681

682 **Figure Legends**

683 **Figure 1 Time-course ion concentration (mg DW^{-1}) in NIL-T and NIL-S leaves during 10**
684 **days 100 mmol L^{-1} NaCl stress.** Na^+ content (**a**), Cl^- content (**b**), K^+ (**c**) content, and K^+ to
685 Na^+ ratio (**d**) in leaves of NIL-T (blue data) and NIL-S (red data). Dry weight of different
686 tissues (**e**) and all tissues (**f**). Observations are means of four replicates ± SEM. Asterisks
687 indicates a significant difference between NIL-T and NIL-S at $*p < 0.05$, $**p < 0.01$ according
688 to the LSD test. DW, dry weight.

689 **Figure 2 Ion concentration in different tissues of NIL-T and -S after 4 days of 100 mmol**
690 **L^{-1} NaCl treatment.** (**a**) Tissue content of Na^+ in leaf, hypocotyl and root of NILs. (**b**) K^+
691 content in leaf, hypocotyl and root of NILs. (**c**) Cl^- content in leaf, hypocotyl and root of NILs.
692 (**d**) NO^{3-} content, Cl^- content and Cl^-/NO^{3-} ratio in leaf and root of NILs. Ion contents are
693 expressed as tissue dry weight. Data are means of 3-5 replicates ± SE. Asterisks indicate a
694 significant difference between NIL-T (blue) and NIL-S (red) at $*p < 0.05$, $**p < 0.01$ according
695 to the LSD test (ion content data in control plants with water supply can be found in Figure
696 S4). FL, first trifoliate leaves; YL, youngest trifoliate leaves; FLP, first trifoliate leaves petiole;
697 YLP, youngest trifoliate leaves petiole; HS, higher stem; LS, lower stem; PR, primary root;
698 SR, secondary root; Hy, hypocotyl. Data shown in (**a**), (**b**), and (**c**) were from one of the two
699 independent experiments with similar results. Data shown in (**d**) were from a separate
700 experiment and repeated twice.

701 **Figure 3 Ion concentration in NIL-T and -S stem phloem and xylem sap after 4 days of**
702 **100 mmol L^{-1} NaCl stress.** (**a**) Na^+, K^+, or Cl^- content to glutamine ratio in NIL-T and NIL-S
703 stem phloem sap. (**b**) Na^+, K^+, and Cl^- concentrations in NIL-T (blue) and NIL-S (red) stem
704 xylem sap. Data are means of three replicates ± SEM. Asterisks indicate a significant difference
705 between NIL 820-T and 820-S at $*p < 0.05$, $**p < 0.01$ according to the LSD test. SPS, stem
706 phloem sap; SXS, stem xylem sap. Data shown here were from one of the three independent
707 experiments with similar results.

708 **Figure 4 Functional test of *GmSALT3* in *E. coli*.** *E. coli* strain TK2463 (defective in
709 potassium uptake, Trk, Kup, and Kdp) harbouring a modified pET-DEST42 vector with
710 *GmSALT3, Gmsalt3, CBL1n, GmSALT3-YFP, GmSALT3-TM10, AtCHX20 and AtKAT1* were
711 grown in different media. (**a**) Low potassium medium (10 g/L tryptone, 2 g/L yeast extract,
712 100 mM D-mannitol; ~2 mM K^+) with additional 0.5 mM Isopropyl β- D-1-
713 thiogalactopyranoside (IPTG). All the test media were supplemented with 100 μg/ml
714 carbenicillin. OD_{600} was monitored every 15 min in 96-well microplate reader. Bars are mean
715 ± SEM of 3 replicates. Growth rates (OD_{600} per hour) of *E.coli* cells within the log phase are

716 indicated between dotted lines, and their slopes are shown in (**b**) (low potassium medium with
717 IPTG). Different letters indicate statistically significant differences between *E. coli* cells
718 harbouring different constructs (one-way ANOVA followed by Fisher's LSD test, $p < 0.05$).
719 **Figure 5 Functional characterization of *GmSALT3* in *X. laevis* oocytes. (a)** Plasma
720 membrane localisation of expressed *GmSALT3-YFP* in oocytes. H_2O-injected and *TmHKT1;5-*
721 *A*-YFP (positive control) expressed oocytes are also shown. Scale bar = 0.5 mm. Oocytes were
722 analysed by confocal laser-scanning microscopy. (**b**) Resting membrane potentials of
723 *GmSALT3*- and H_2O-injected oocytes after incubation in ND96 for 72 hours. Values are means
724 ± SEM (n = 8), Asterisks indicate a significant difference between GmSALT3- and H_2O-
725 injected oocytes at $*p < 0.01$ according to the LSD test. (**c**) Net ion fluxes were measured on
726 oocytes plasma membrane using MIFE (Microelectrode Ion Flux Estimation). Oocytes were
727 incubated in ND96 for 72 hours, and washed in ND96 in (96 mM NaCl, 1 mM KCl, 1 mM
728 $MgCl_2$, 5 mM HEPES, pH 7.5). Measurements were done in BSM (Basal Salty Medium; 5 mM
729 NaCl, 0.2 mM KCl, 0.2 mM $CaCl_2$, 5 mM HEPES, pH 7.5) and exchanged after time zero to
730 BSM with sufficiently low concentrations of Na^+, K^+ and Cl^- to ensure a gradient for efflux for
731 target ions and an improved signal:noise ratio. Values are means ± SEM (n = 4 - 6). (**d**) Ion
732 (Na^+, K^+, and Cl^-) concentrations in *GmSALT3* (blue) and H_2O (Red) injected oocytes after
733 incubation in ND96 (72 hours), BSM (overnight), BSM with 100 µM amiloride (overnight).
734 Values are means ± SEM (n = 4-7). Asterisks indicate a significant difference between
735 *GmSALT3*-injected and H_2O-injected oocytes at $*p < 0.05$, $**p < 0.01$ according to the LSD
736 test.
737
738
739
740
741
742
743
744
745
746

747 **Supporting Information**

748 **Fig. S1. Time-course ion concentration (Na^+) in NIL 820-T and 820-S leaves, stems,**
749 **hypocotyls, and roots during 10 days NaCl stress.**

750 **Fig. S2. Time-course ion concentration (K^+) in NIL 820-T and 820-S leaves, stems,**
751 **hypocotyls, and roots during 10 days NaCl stress.**

752 **Fig. S3. Time-course ion concentration (Cl^-) in NIL 820-T and 820-S leaves, stems,**
753 **hypocotyls, and roots during 10 days NaCl stress.**

754 **Fig. S4. Ion content and ion flux in NIL 820-T and 820-S different tissues after 4 days in**
755 **control conditions.**

756 **Fig. S5. Ultrastructure of NIL-*GmSALT3* and NIL-*Gmsalt3* root cross sections with 4 days**
757 **NaCl stress.**

758 **Fig. S6. Functional test of *GmSALT3* in *E. coli* with low potassium and KML medium**.

759 **Table S1. Primers used in this study. Primers were designed and adjusted using Primer3.**

760
761
762
763
764

765 **Figures**

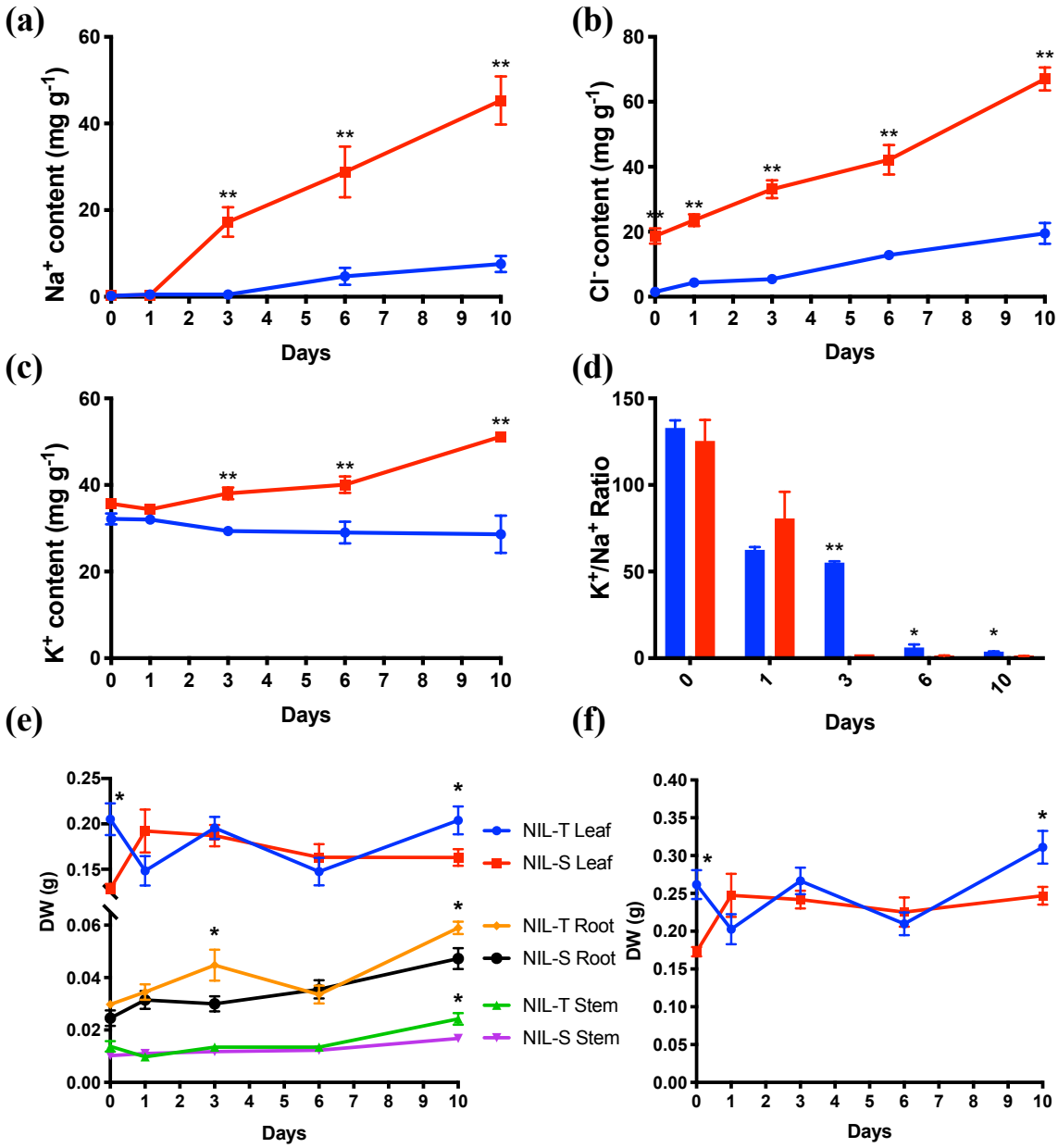

766

767 **Figure 1 Time-course ion concentration (mg DW^{-1}) in NIL-T and NIL-S leaves during 10**
768 **days 100 mmol L^{-1} NaCl stress.** Na^+ content (**a**), Cl^- content (**b**), K^+ (**c**) content, and K^+ to
769 Na^+ ratio (**d**) in leaves of NIL-T (blue data) and NIL-S (red data). Dry weight of different
770 tissues (**e**) and all tissues (**f**). Observations are means of four replicates ± SEM. Asterisks
771 indicates a significant difference between NIL-T and NIL-S at *p <0.05, **p < 0.01 according
772 to the LSD test. DW, dry weight.

773

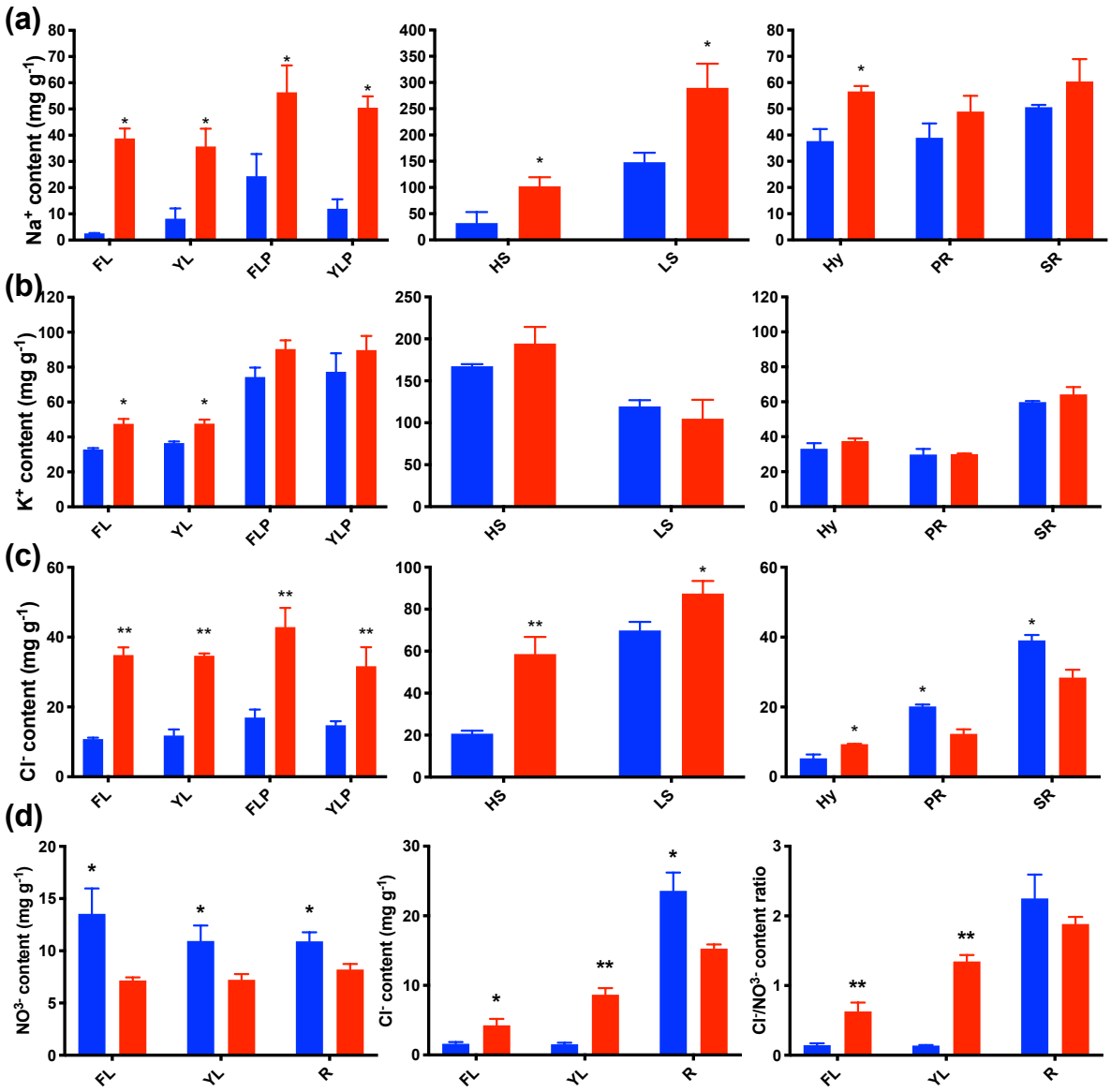

Figure 2 Ion concentration in different tissues of NIL-T and -S after 4 days of 100 mmol L^{-1} NaCl treatment. (**a**) Tissue content of Na^+ in leaf, hypocotyl and root of NILs. (**b**) K^+ content in leaf, hypocotyl and root of NILs. (**c**) Cl^- content in leaf, hypocotyl and root of NILs. (**d**) NO^{3-} content, Cl^- content and Cl^-/NO^{3-} ratio in leaf and root of NILs. Ion contents are expressed as tissue dry weight. Data are means of 3-5 replicates ± SE. Asterisks indicate a significant difference between NIL-T (blue) and NIL-S (red) at $*p < 0.05$, $**p < 0.01$ according to the LSD test (ion content data in control plants with water supply can be found in Figure S4). FL, first trifoliate leaves; YL, youngest trifoliate leaves; FLP, first trifoliate leaves petiole; YLP, youngest trifoliate leaves petiole; HS, higher stem; LS, lower stem; PR, primary root; SR, secondary root; Hy, hypocotyl. Data shown in (**a**), (**b**), and (**c**) were from one of the two independent experiments with similar results. Data shown in (**d**) were from a separate experiment and repeated twice.

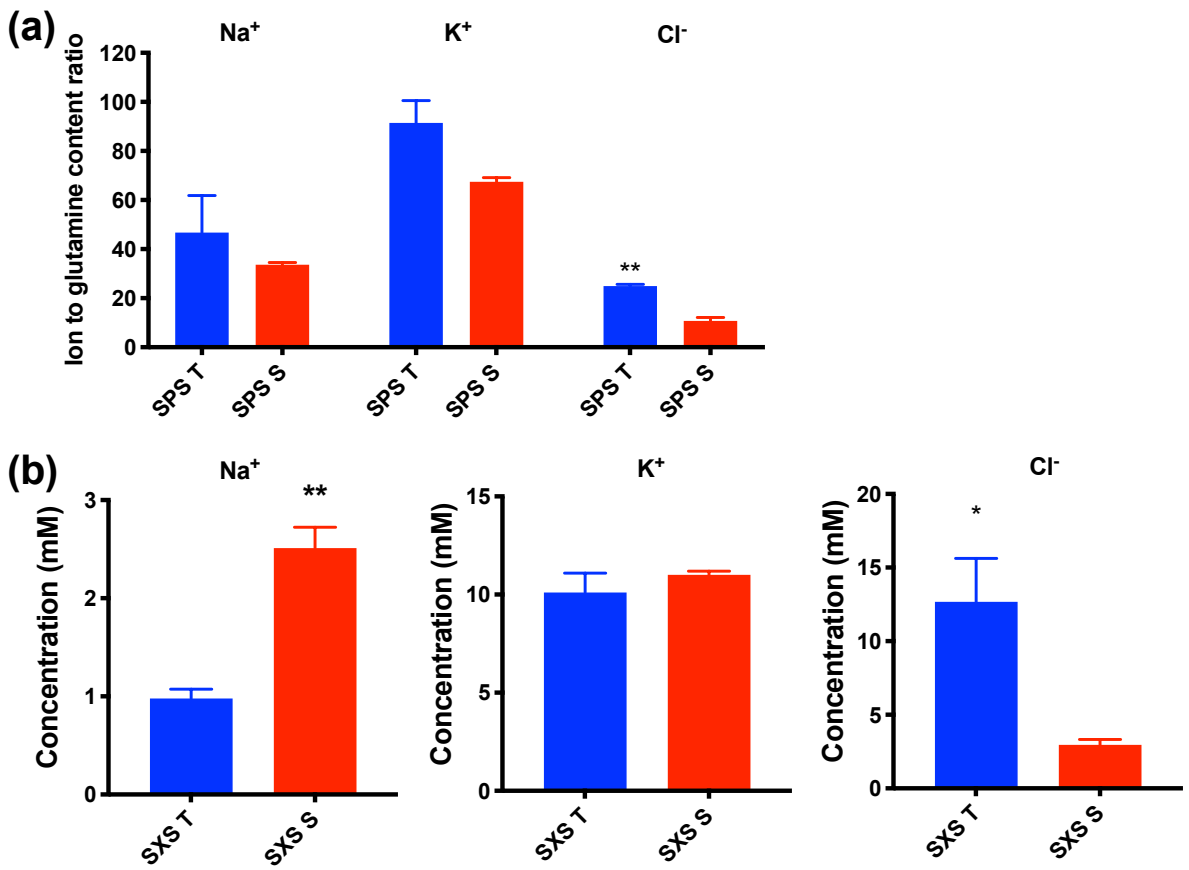

Figure 3 Ion concentration in NIL-T and -S stem phloem and xylem sap after 4 days of 100 mmol L^{-1} NaCl stress. **(a)** Na^+, K^+, or Cl^- content to glutamine ratio in NIL-T and NIL-S stem phloem sap. **(b)** Na^+, K^+, and Cl^- concentrations in NIL-T (blue) and NIL-S (red) stem xylem sap. Data are means of three replicates ± SEM. Asterisks indicate a significant difference between NIL 820-T and 820-S at *p <0.05, **p < 0.01 according to the LSD test. SPS, stem phloem sap; SXS, stem xylem sap. Data shown here were from one of the three independent experiments with similar results.

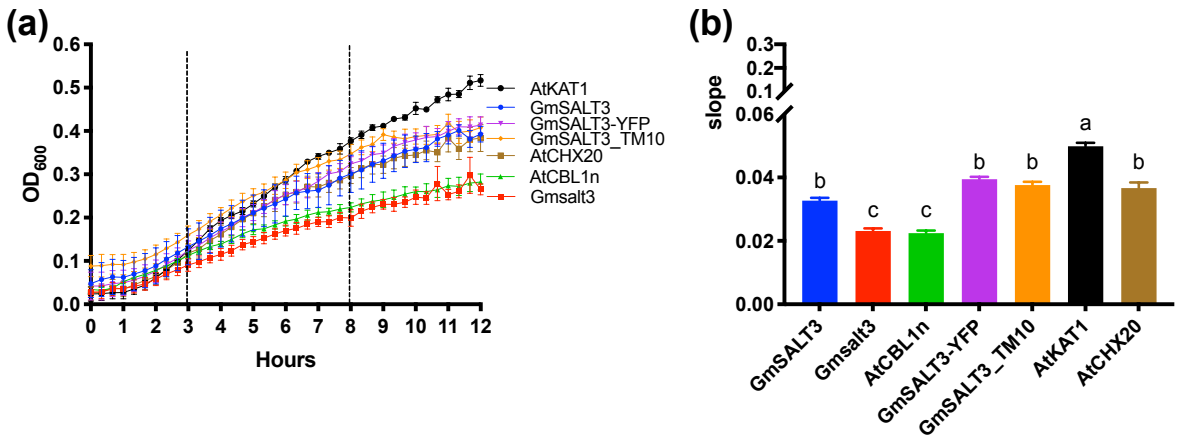

802

803 **Figure 4 Functional test of *GmSALT3* in *E. coli*.** *E. coli* strain TK2463 (defective in
804 potassium uptake, Trk, Kup, and Kdp) harbouring a modified pET-DEST42 vector with
805 *GmSALT3, Gmsalt3, CBL1n, GmSALT3-YFP, GmSALT3-TM10, AtCHX20 and AtKAT1* were
806 grown in different media. (**a**) Low potassium medium (10 g/L tryptone, 2 g/L yeast extract,
807 100 mM D-mannitol; ~2 mM K^+) with additional 0.5 mM Isopropyl β- D-1-
808 thiogalactopyranoside (IPTG). All the test media were supplemented with 100 μg/ml
809 carbenicillin. OD_{600} was monitored every 15 min in 96-well microplate reader. Bars are mean
810 ± SEM of 3 replicates. Growth rates (OD_{600} per hour) of *E.coli* cells within the log phase are
811 indicated between dotted lines, and their slopes are shown in (**b**) (low potassium medium with
812 IPTG). Different letters indicate statistically significant differences between *E. coli* cells
813 harbouring different constructs (one-way ANOVA followed by Fisher's LSD test, $p < 0.05$).

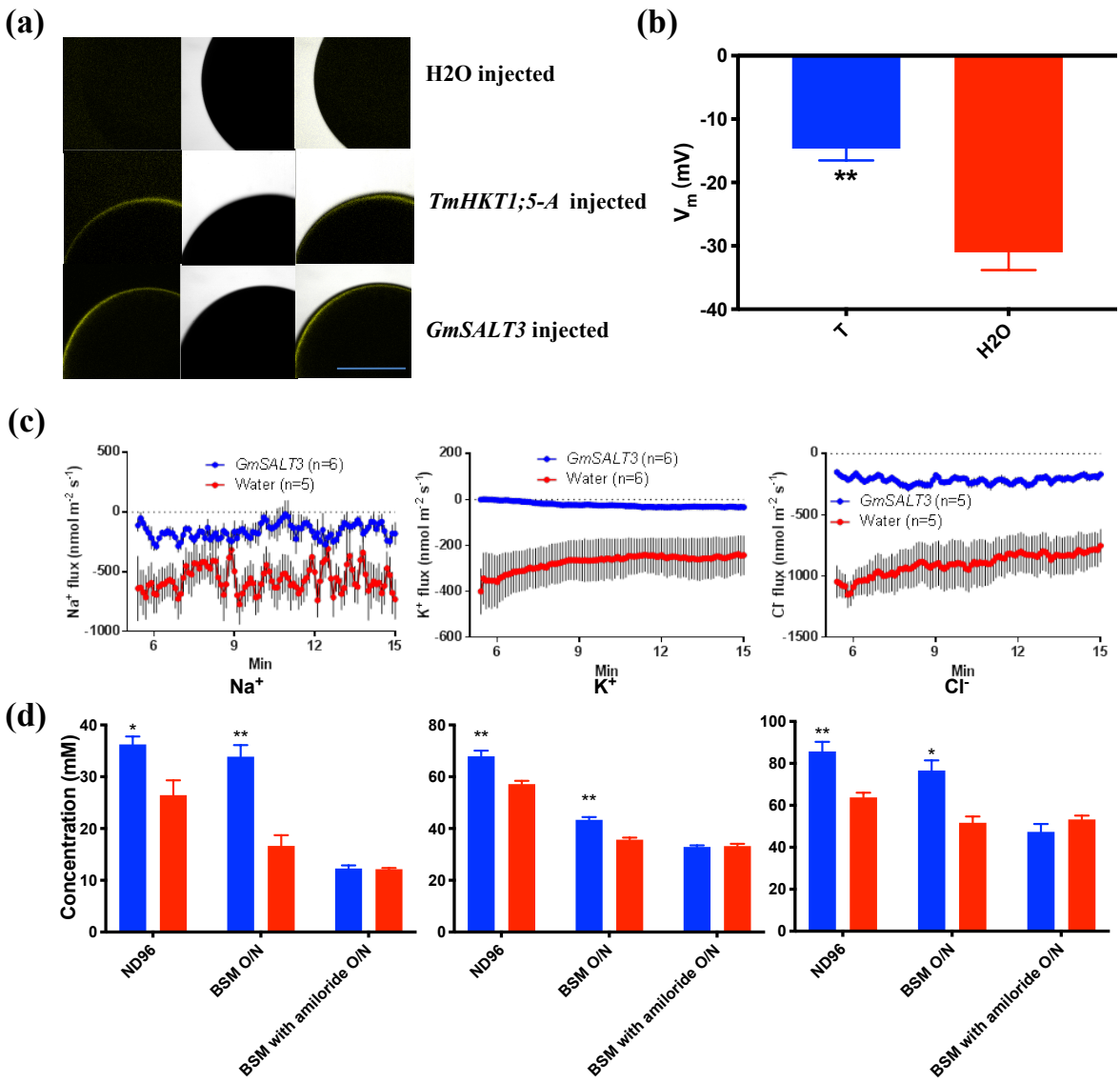

Figure 5 Functional characterization of *GmSALT3* in *X. laevis* oocytes. (a) Plasma membrane localisation of expressed *GmSALT3-YFP* in oocytes. H_2O-injected and *TmHKT1;5-A*-YFP (positive control) expressed oocytes are also shown. Scale bar = 0.5 mm. Oocytes were analysed by confocal laser-scanning microscopy. **(b)** Resting membrane potentials of *GmSALT3*- and H_2O-injected oocytes after incubation in ND96 for 72 hours. Values are means ± SEM (n = 8), Asterisks indicate a significant difference between GmSALT3- and H_2O-injected oocytes at $*p < 0.01$ according to the LSD test. **(c)** Net ion fluxes were measured on oocytes plasma membrane using MIFE (Microelectrode Ion Flux Estimation). Oocytes were incubated in ND96 for 72 hours, and washed in ND96 in (96 mM NaCl, 1 mM KCl, 1 mM $MgCl_2$, 5 mM HEPES, pH 7.5). Measurements were done in BSM (Basal Salty Medium; 5 mM NaCl, 0.2 mM KCl, 0.2 mM $CaCl_2$, 5 mM HEPES, pH 7.5) and exchanged after time zero to BSM with sufficiently low concentrations of Na^+, K^+ and Cl^- to ensure a gradient for efflux for

827 target ions and an improved signal:noise ratio. Values are means ± SEM (n = 4 - 6). (**d)** Ion
828 (Na^+, K^+, and Cl^-) concentrations in *GmSALT3* (blue) and H_2O (Red) injected oocytes after
829 incubation in ND96 (72 hours), BSM (overnight), BSM with 100 μM amiloride (overnight).
830 Values are means ± SEM (n = 4-7). Asterisks indicate a significant difference between
831 *GmSALT3*-injected and H_2O-injected oocytes at $*p < 0.05$, $**p < 0.01$ according to the LSD
832 test.
833
834